Phys. Med. Biol. 39 (1994) 381–387. Printed in the UK

Oversampled filters for quantitative volumetric PET reconstruction

Charles W Stearns, Carl R Crawford and Hui Hu
Applied Science Laboratory, GE Medical Systems, Milwaukee, WI 53201, USA

Received 13 October 1993

Abstract. Three-dimensional filtered backprojection uses filters generally specified in the Fourier domain. Implementing these filters by direct sampling in the Fourier domain produces an artifact in the reconstructed images consisting primarily of a DC shift. This artifact is caused by aliasing of the reconstruction filter. We have developed a filter construction technique using Fourier domain oversampling, which reduces the artifact. A method to construct the filter efficiently without the need to create and store the entire oversampled filter array is also presented. Quantitative accuracy in filtered backprojection is of particular importance in multiple-pass algorithms used to reconstruct data from cylindrical PET scanners. We are able to implement such algorithms without fitting the reprojected views to the scanner data.

1. Introduction

Artifacts, consisting of an image amplitude shift and low-frequency shading, occur in two-dimensional filtered backprojection when the band-limited ramp filter is sampled directly in the Fourier domain (Kak and Slaney 1988, Crawford 1991). These artifacts are absent when the filter is computed in the space domain. The artifacts are caused by aliasing that occurs because the inverse Fourier transform of the filter, its point spread function, has infinite extent. The magnitude of the shift is proportional to the integrated amplitude of the imaged object.

The filters used in three-dimensional filtered backprojection, such as those developed by Colsher (1980), must also be band limited to implement the reconstruction with sampled data. If the filters are sampled in the Fourier domain, a similar shift artifact will be expected in the reconstructed image. In this paper we demonstrate this shift artifact in images reconstructed using filters sampled in the Fourier domain.

While a shift artifact is detrimental to any quantitative image reconstruction, it is of particular concern in PET reconstructions using the two-pass algorithm originally suggested by Pelc (1979) and implemented by Kinahan and Rogers (1989), since this algorithm utilizes data estimated from a reconstructed image to complete the truncated projection views. Even a small DC shift in the preliminary image would create a large shift in the forward-projected views used by the algorithm. Previously reported implementations of this algorithm have included a linear regression step to determine a scale factor and offset to align the forward-projected information to the scanner data (Townsend *et al* 1991, Cherry *et al* 1991).

There are several methods to eliminate this artifact in two-dimensional reconstruction, which could be extended to three-dimensional reconstruction. Kak and Slaney (1988) and Crawford (1991) compute the filter in the space domain, then transform the filter to the Fourier domain for efficient implementation of the filtering operation. Crawford (1991)

0031-9155/94/030381+07$19.50

derives correction factors for the low-frequency terms of the filter based on the aliased portions of the point spread function. Both of these methods require a closed-form space domain representation of the reconstruction filter. Although Kinahan *et al* (1988) have presented the space domain representation of the Colsher filter, and Defrise *et al* (1993) have determined filters for a large class of valid reconstruction filters, their equations contain singularities, which make practical implementation impossible. This paper presents an alternative filter construction method that effectively eliminates the image artifact.

2. Theory

We extend the description of the shift artifact in 2D image reconstruction by Crawford (1991) to 3D image reconstruction. Consider the task of filter the 2D projection $p(u, v)$, which is sampled at an interval a in the u-direction and b in the v-direction. The projection of the imaged object is contained within an $(M/2 \times N/2)$ pixel region on $p(u, v)$. Although we may implement the convolution as a pointwise multiplication in the Fourier domain, an accurate reconstruction requires that $p(u, v)$ be convolved with a filter function $h(u, v)$, where $h(u, v)$ is the inverse transform of the reconstruction filter $H(r, s)$. Since $p(u, v)$ is sampled, $H(r, s)$ is band limited in frequency to $r \leqslant |1/2a|, s \leqslant |1/2b|$. An $(M \times N)$-point set of samples of the filter function is required to avoid circular convolution artifacts in the filtering of the projection (this is an extension of the 1D filtering result presented by Kak and Slaney (1988)):

$$h'(i, j) = h(ia, jb) \tag{1}$$

where $-(M/2) \leqslant i < (M/2)$ and $-(N/2) \leqslant j < (N/2)$. In practice, M and N are usually extended to the next power of two and the fast Fourier transform (FFT) is used.

Since, as previously stated, $h(u, v)$ is unavailable, the FFT of $h'(i, j)$, $H'(\omega_i, \omega_j)$, must be obtained by another means. Direct sampling of $H(r, s)$, defined by the equation

$$H_{\text{samp}}(\omega_i, \omega_j) = H(\omega_i/aM, \omega_j/bN) \tag{2}$$

where $-(M/2) \leqslant \omega_i < (M/2)$ and $-(N/2) \leqslant \omega_j < (N/2)$, produces a filter response which is an aliased version of the desired point spread function:

$$h_{\text{samp}}(i, j) = \text{FFT}^{-1}\{H_{\text{samp}}(\omega_i, \omega_j)\} = \sum_{\alpha=-\infty}^{\infty} \sum_{\beta=-\infty}^{\infty} h((i + \alpha M)a, (j + \beta N)b). \tag{3}$$

One term of this series, $\alpha = \beta = 0$, is the desired point spread response $h'(i, j)$; the other terms contribute aliasing to the filter.

The magnitude of $h(u, v)$ decreases quickly away from the origin; Kinahan *et al* (1988) have demonstrated a $-1/r^3$ dependence for the Colsher filter. If the values of M and N in equation (3) are increased, the aliasing caused by the $\alpha \neq 0, \beta \neq 0$ terms, while not eliminated, will have less impact on $h(i, j)$. This 'oversampling' of the filter array is accomplished by sampling $H(r, s)$ more densely. Oversampling $H(r, s)$ by a factor of k produces the array

$$H_k(\omega_i, \omega_j) = H(\omega_i/akM, \omega_j/bkN) \tag{4}$$

where $-(kM/2) \leqslant \omega_i < (kM/2)$ and $-(kN/2) \leqslant \omega_j < (kN/2)$. The inverse transform of the oversampled filter is

$$h_k(i, j) = \sum_{\alpha=-\infty}^{\infty} \sum_{\beta=-\infty}^{\infty} h((i + \alpha kM)a, (j + \beta kN)b) \tag{5}$$

for $-(kM/2) \leqslant i < (kM/2)$ and $-(kN/2) \leqslant j < (kN/2)$.

Like h_{samp} above, h_k is still aliased, but the aliasing effect will be decreased. We have found that oversampling by a factor of four makes the central $M \times N$ points of h_k a sufficient estimate of $h'(i, j)$ for the purposes of PET reconstruction.

3. Methods

The steps to generate an $M \times N$ filter by oversampling are as follows:

(i) oversample the filter in the Fourier domain by a factor of k, producing a Fourier domain filter array of dimension $kM \times kN$;

(ii) take the inverse 2D FFT of the oversampled filter to form a space domain array of dimension $kM \times kN$;

(iii) extract a subarray containing the $M \times N$ points centred at the origin; and

(iv) to implement the filtering operation in the Fourier domain, take the 2D FFT of the subarray to produce the final Fourier domain filter array.

Direct implementation of the oversampling technique may be hampered by the size of the oversampled filter array; if $M = 512$, $N = 128$ and $k = 4$, the oversampled array has 2^{20} elements. In addition, most of the $kM \times kN$ space domain array need not be computed, since only an $M \times N$ portion of the array is required. Fortunately, decimation of the Fourier transform equation may be used to reduce the computation and storage requirements for the oversampling algorithm. We use a 2D variation of the transform decomposition method described by Sorensen and Burrus (1993) for the 1D FFT.

To demonstrate the decimation technique, define the desired space domain subarray to be $h(u, v)$, $0 \leqslant u < M$ and $0 \leqslant v < N$, and the oversampled filter array to be $H(r, s)$, $0 \leqslant r < kM$ and $0 \leqslant s < kN$. Because the filters under consideration are all real and symmetric across both axes, it is only necessary to compute $h(u, v)$ over one-quarter of the array area, where $0 \leqslant u < M/2$ and $0 \leqslant v < N/2$.

The inverse transform of the oversampled filter is given by the equation

$$h(u, v) = \frac{1}{k^2MN} \sum_{r=0}^{kM-1} \sum_{s=0}^{kN-1} H(r, s) W_{kM}^{-ru} W_{kN}^{-sv} \tag{6}$$

where $W_Z = \mathrm{e}^{(-j2\pi/Z)}$. Consider the substitution

$$s = (2k)c + d \qquad 0 \leqslant c < N/2 \qquad 0 \leqslant d < 2k \tag{7}$$

which yields

$$h(u, v) = \frac{1}{2k} \sum_{d=0}^{2k-1} W_{kN}^{-dv} \left\{ \frac{2}{N} \sum_{c=0}^{N/2-1} W_{N/2}^{-cv} \left(\frac{1}{kM} \sum_{r=0}^{kM-1} H(r, 2kc + d) W_{kM}^{-ru} \right) \right\}. \tag{8}$$

The portion in round brackets is the kM-point inverse FFT (IFFT) of the $(2kc + d)$th row of the oversampled filter; the portion in curly brackets is the $(N/2)$-point IFFT of a column of pixels drawn from those row inverse transforms.

The following algorithm computes $h(u, v)$ for $0 \leqslant u < M/2$ and $0 \leqslant v < N/2$ based on equation (8).

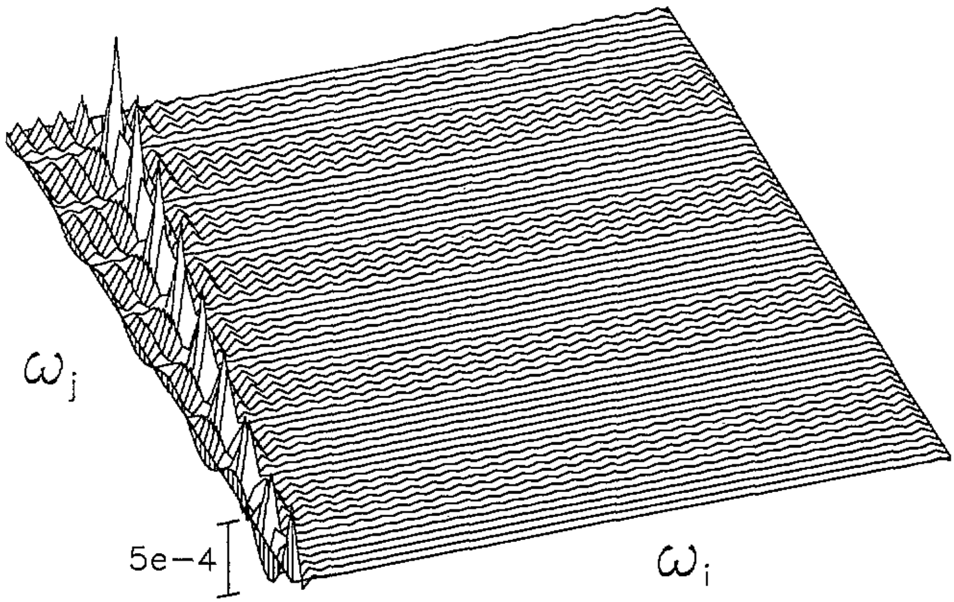

Figure 1. One quadrant of the difference between a Colsher filter (axial angle of 4°; maximum angle of 9°) computed by direct Fourier domain sampling and fourfold oversampling.

(i) Create an $M/2 \times N/2$ real array h, an $M/2 \times N/2$ complex array S (a scratch buffer), and a kM-element real vector H. Zero array h.

(ii) For each d from zero to $2k - 1$

— for each c from zero to $N/2 - 1$

(a) create the $(2kc + d)$th row of the oversampled filter in vector H,
(b) take the IFFT of H, and
(c) place the first $M/2$ complex values of the transformed H into the cth row of S and

— for each u from zero to $M/2 - 1$

(a) take the IFFT of the uth column of S and
(b) for each v from zero to $N/2-1$, multiply the vth element of the transformed column data by $(1/2k)W_{kM}^{-dv}$, and add the real portion to $h(u, v)$.

The total storage requirement for h, S and H in this algorithm is $\frac{3}{4}MN + kM$ floating point numbers, compared to the k^2MN floating point numbers required to store the H array in the direct implementation. At this point, the one computed quadrant of $h(u, v)$ is copied and reflected to fill the full $h(u, v)$ array, and its forward $(M \times N)$-point 2D FFT is taken to determine the Fourier domain filter for use in the reconstruction algorithm.

4. Results

Figure 1 is a surface plot of the difference between a Colsher filter generated by direct Fourier sampling and by fourfold oversampling. The greatest difference between the two

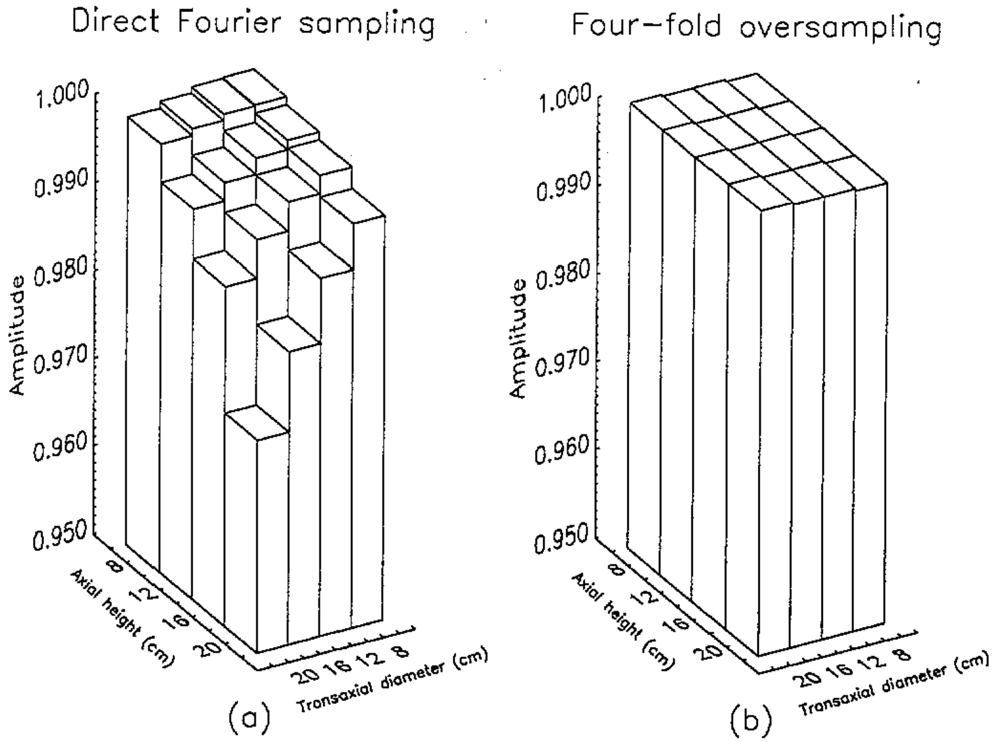

Figure 2. Relative image amplitude at object centre for a set of cylinders reconstructed using Colsher filters created by (*a*) direct Fourier sampling and (*b*) fourfold oversampling. The transaxial diameter (right axis) and axial height (left axis) of the cylinder are varied.

filters occurs near the origin and near the line on the filter plane corresponding to where the Fourier domain slice representing the projection intersects the double cone defined by the maximum acceptance angle. This is expected, since the filter has discontinuities in its slope at these locations.

Sixteen different volumetric projection data sets (five circles of projection planes spaced by 2°, 128 views per circle; 63×63 points per projection plane, sampled spaced by 0.52 cm in each direction) were calculated for cylindrical objects whose diameters and heights ranged from 8 cm to 20 cm. Each cylinder was centred in the imaging field of view, and each was fully viewed in all projection planes. The data sets were reconstructed using Colsher filters created by direct Fourier sampling and also by fourfold oversampling onto an image grid of 0.5 cm voxels. The average voxel value in a 7×7 voxel region at the centre of the central image plane of each reconstructed image was calculated to determine the degree of shift artifact present in the reconstructed image. The results using directly sampled filters are shown in figure 2(a). Each of the reconstructed images has a negative amplitude shift relative to that of the smallest cylinder. Increases in cylinder size, either diameter or height, worsen the shift in the reconstructed image. The largest cylinder exhibited a shift of -2.6% relative to the smallest object. The results using the oversampled filters are shown in figure 2(b). There is no amplitude shift at the scale shown among the reconstructed objects; all recovery values were equal to within 0.1%.

Using the oversampling technique, and taking appropriate care to preserve the

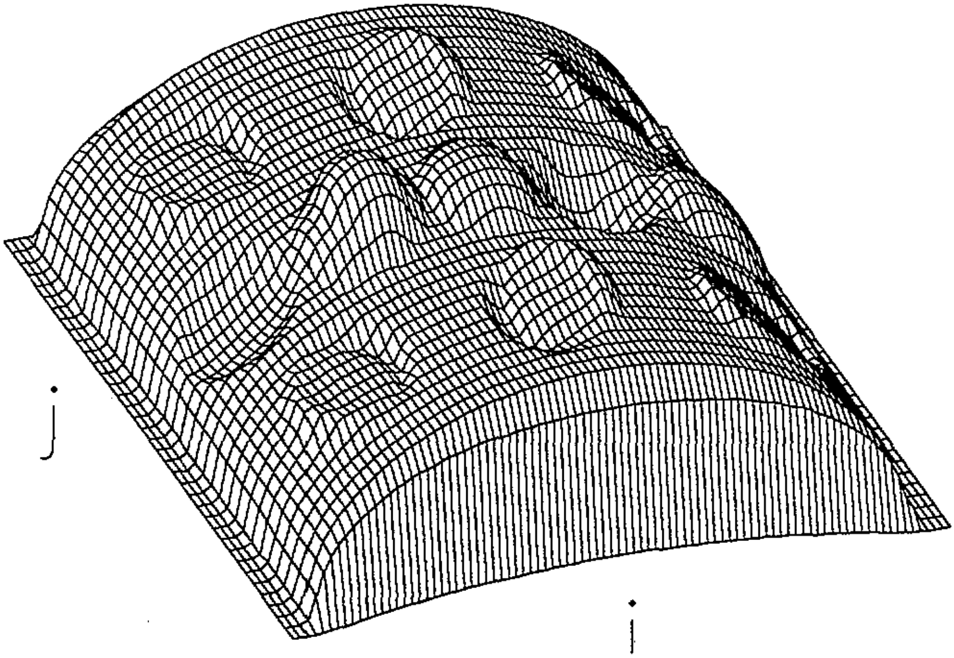

Figure 3. One completed projection plane from a Kinahan and Rogers reconstruction of a simulated cylindrical phantom with several contrasting inserts. The central 27 rows of the array are simulated scanner data; the top five and bottom five rows are reprojected from a preliminary reconstruction of the phantom.

multiplicative constants in the filtering process, we are able to generate images from which reprojected data can be estimated without the need for a fitting step to take place. Figure 3 shows a surface plot of a completed projection view of a simulated cylindrical phantom containing several spheres of positive and negative contrast. The projection contains 89×37 pixels; the central 27 rows are simulated projection data, the top five and bottom five rows are reprojected from a preliminary image of the phantom reconstructed using filters constructed by fourfold oversampling. If there were a shift artifact in the preliminary image, a discontinuity would be expected at the boundary between the projected and the reprojected data. Since no such discontinuity is seen, we can proceed with the full 3D reconstruction of the phantom without a fitting step.

5. Conclusion

Direct Fourier domain sampling of the reconstruction filters used in 3D filtered backprojection produces an image artifact consisting primarily of a DC shift in the output image. This artifact is caused by aliasing of the point spread response of the reconstruction filter. Constructing the filter by the oversampling technique described here reduces the artifact. We have found that oversampling by a factor of four effectively eliminates the artifact. A method to construct the filter efficiently without the need to create and store the entire oversampled filter array has been presented. Using oversampled filters, we are able to implement the

Kinahan and Rogers reconstruction algorithm without fitting the reprojected views to the scanner data.

References

Cherry, S R, Dahlbom M and Hoffman E J 1991 3D PET using a conventional multislice tomograph without septa *J. Comput. Assist. Tomogr.* **15** 655–68

Colsher J G 1980 Fully three-dimensional positron emission tomography *Phys. Med. Biol.* **20** 103–15

Crawford C R 1991 CT filtration aliasing artifacts *IEEE Trans. Med. Imaging* **MI-10** 92–102

Defrise M, Clack R and Townsend D 1993 Solution to the three-dimensional image reconstruction problem from two-dimensional parallel projections *J. Opt. Soc. Am.* A **10** 869–77

Kak A C and Slaney M 1988 *Principles of Computerized Tomographic Imaging* (New York: IEEE) pp 69–77

Kinahan P E and Rogers J G 1989 Analytic three-dimensional image reconstruction using all detected events *IEEE Trans. Nucl. Sci.* **NS-36** 964–8

Kinahan P E, Rogers J G, Harrop R and Johnson R R 1988 Three-dimensional image reconstruction in object space *IEEE Trans. Nucl. Sci.* **NS-35** 635–8

Pelc N J 1979 A generalized filtered backprojection reconstruction algorithm *ScD Thesis* Harvard School of Public Health

Sorensen H V and Burrus C S 1993 Efficient computation of the DFT without only a subset of input or output points *IEEE Trans. Acoust. Speech, Signal Process.* **ASSP-41** 1184–200

Townsend D W, Geissbuhler A, Defrise M, Hoffman E J, Spinks T L, Bailey D L, Gilardi M-C and Jones T 1991 Fully three-dimensional reconstruction for a PET camera with retractable septa *IEEE Trans. Med. Imaging* **MI-10** 505–12